Development of methods for material properties identification in composite structures

André Filipe Ferreira Rodrigues
andre.f.f.rodrigues@tecnico.ulisboa.pt

Instituto Superior Técnico, Universidade de Lisboa, Portugal

January 2021

Abstract

This work proposes a non-destructive method for the identification of material properties of composite materials. This method takes advantage of the simulation capabilities of ANSYS® software, using ANSYS® Parametric Design Language (APDL) to perform modal analyses and extract natural frequencies of the specimens. ANSYS® and MATLAB® are integrated to solve several optimisation problems. The proposed optimisation problems have for design variables the material elastic constants and make use of Nature-inspired metaheuristic optimisation algorithms to evaluate an objective function using a derivative-free method. These objective functions relate experimental natural frequencies, which are extracted from numerous studies carried out in the past by other authors, with computationally obtained ones. The Nature-inspired metaheuristic optimisation algorithms tested are the Genetic algorithm, the Particle Swarm Optimisation algorithm, the Grey Wolf Optimisation algorithm, the Firefly Algorithm and Cuckoo Search algorithm. The different search agents population generated by the algorithms search the available space looking for the global minimum of the objective function, independently of the initial population position in the search space. The proposed method is applied to several specimens of different materials either they are constructed with synthetic fibres, such as glass fibres, or natural fibres, such as wood fibres and plywood. This method proved to obtain the material elastic constants within an acceptable range compared to other methods, provided that enough natural frequencies are accurately measured and provided.

Keywords: Composite Materials, Green composites, Material Properties, Elastic constants, Nature-inspired optimisation

1. Introduction

The automotive and aerospace industries' urge to develop new lighter vehicles with a smaller biological blueprint boosted the development of new materials. These new materials have better mechanical properties than the existing ones. To achieve this, engineers developed what is known as composite materials.

These new composite materials are tailored to the specific need of each project. The most common used materials in composites are carbon fibres, glass fibres and aramid fibres obtained from non-renewable sources. Therefore, searching for renewable materials sources is essential; materials like wood, jute straw and flax can easily be processed into natural fibres that are transformed in what is called green composites.

Green composites or natural fibre composites combine natural fibres with a polymeric matrix; this allows the use of several combinations of materials to achieve the desired properties.

During the design of structures or structural components, materials with specific properties are needed. Therefore, new composite materials are created in order to meet design requirements. As a consequence, it is imperative to assess the mechanical properties of these composite materials. Considering that composite materials are heterogeneous by nature, to fully determine all the mechanical properties, it is necessary to perform a vast number of tests, which have a cost. In this work, a non-destructive method for properties identification is developed. It relies on commercial software to easily estimate the mechanical properties of the specimen in the study. Meta-heuristic nature-inspired optimisation algorithms are used to minimise an error function relating experimental and computational modal parameters.

This work focuses on studying laminated composite materials, whether they are synthetic fibre reinforced, such as glass fibres reinforced composites, or they are natural fibres reinforced like wooden fibres reinforced composites and plywood. However, a specimen of aluminium is also analysed to establish a baseline and test the proposed method.

2. Background

2.1. Historical Overview

The first use of the metaheuristic method and metaheuristic algorithms is difficult to pinpoint in history, although its importance is well established in the scientific community nowadays. The development of more powerful computers drives the development of new, more efficient algorithms. One hundred and ninety-two metaheuristic algorithms are listed in M. Almufti [1] and seventy four nature-inspired metaheuristic algorithms in Fister et al. [2].

Nature-inspired algorithms gained popularity in the scientific community due to their efficiency to evaluate an objective function. They use stochastic ideas and random numbers, given the design variables and constraints, to evaluate an objective func-

tion. These algorithms evaluate the function using a derivative-free method, thus not requiring the calculation of analytical or numerical derivatives of the objective function. Another characteristic that makes these methods so attractive is that they can be applied to any function because they only evaluate the function values.

Despite the benefits described above, nature-inspired algorithms also have some drawbacks. These algorithms may require a large sample of objective function evaluations in order to solve the problem. This implies that a large amount of computational power may be necessary to process the data. Additionally, there is no guarantee that a global minimum is obtained, having the possibility instead of finding a local minimum.

2.2. Overview of methods for materials characterisation

Materials are characterised by their engineering constant, also known as elastic constants. Different elastic constants represent different characteristics of the structure. The elastic constants analysed are Young's modulus, E, which relates extensional strain in the direction of loading to stress in the direction of loading; the Poisson's ratio, ν, relates extensional strain in the loading direction to extensional strain in another direction; and the shear modulus, G, relates shear strain in the plane of shear loading to that shear stress [3].

Most of the times, the material properties are determined in a laboratory in terms of engineering constants. These constants are measured using tests like uniaxial tension test. Due to their physical meaning, the engineering constants are used in place of more abstract stiffness coefficients and compliance coefficients, thus the relation between strains and stresses can be written as a function of the engineering constants according to:

$$\begin{Bmatrix} \varepsilon_1 \\ \varepsilon_2 \\ \varepsilon_3 \\ \varepsilon_4 \\ \varepsilon_5 \\ \varepsilon_6 \end{Bmatrix} = \begin{bmatrix} \frac{1}{E_1} & -\frac{\nu_{21}}{E_2} & -\frac{\nu_{31}}{E_3} & 0 & 0 & 0 \\ -\frac{\nu_{12}}{E_1} & \frac{1}{E_2} & -\frac{\nu_{32}}{E_3} & 0 & 0 & 0 \\ -\frac{\nu_{13}}{E_1} & -\frac{\nu_{23}}{E_2} & \frac{1}{E_3} & 0 & 0 & 0 \\ 0 & 0 & 0 & \frac{1}{G_{23}} & 0 & 0 \\ 0 & 0 & 0 & 0 & \frac{1}{G_{13}} & 0 \\ 0 & 0 & 0 & 0 & 0 & \frac{1}{G_{12}} \end{bmatrix} \begin{Bmatrix} \sigma_1 \\ \sigma_2 \\ \sigma_3 \\ \sigma_4 \\ \sigma_5 \\ \sigma_6 \end{Bmatrix} \quad (1)$$

where E_1, E_2, E_3 are the Young's modulus in 1, 2, and 3 material directions, respectively, ν_{ij} is the Poisson's ratio defined as the ratio of the transverse strain in the jth direction to the axial strain in the ith direction when stressed in the ith direction and G_{23}, G_{13}, G_{12} are the shear moduli in the 2-3, 1-3 and 1-2 plane, respectively [4].

The methods for material properties identification can be divided into two classes: methods that use destructive techniques and non-destructive ones, as can be seen in Figure 1.

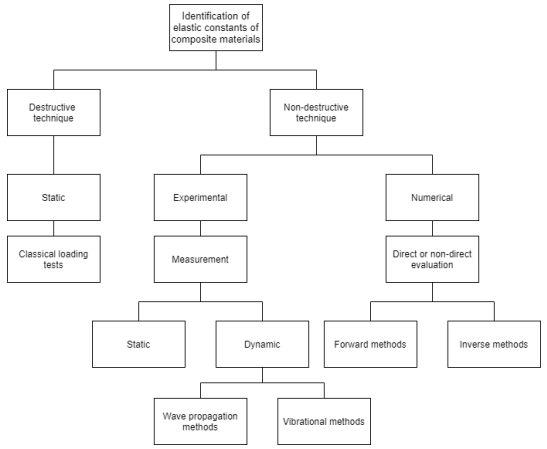

Figure 1: Overview of composite material properties identification methodologies [5].

Non-destructive techniques involve two parts, an experimental and a numerical part, being these techniques most of the times referred to as experimental-numerical techniques [5].

In the experimental part significant parameters are measured and extracted to be later used in the numerical part. Two approaches are considered, the static and the dynamic approach. In the static approach a specimen is subjected to a transverse quasi-static load. The dynamic approach can be divided into the wave propagation method and the vibrational method. The wave propagation method uses an ultrasonic wave travelling through a specimen. The vibrational method makes use of external excitations in order to obtain a frequency response function and extract modal parameters, in particular natural frequencies and mode shapes. The natural frequencies are the frequencies at which a physical structure will tend to vibrate. Natural frequencies depend on the way mass and stiffness are distributed within the structure. Each structure posses its unique set of natural frequencies and mode shapes, which describes how a structure moves at a particular natural frequency.

To fully determine the material properties of a specimens the numerical part of this method can be a direct evaluation, in which the direct identification of elastic properties of a material is obtained from a derived inverse equation with the experimental resonant frequencies as data. Alternatively, it can be a non-direct evaluation, in which the objective is the minimisation or maximisation of objective functions. This last approach involves both forward methods and inverse methods in order to determine the material properties of the composite material.

Soares et al. [6] used the non-direct method to predict material properties of composite plates. In this case, experimentally determined eigenfrequencies of the plate in the study are compared to the corresponding numerical eigenvalues through the use of an objective function and an optimisation technique is applied. The generalisation of this method is presented by Araújo et al. [7], where experimental values of material parameters are determined. The numerical part is replaced by a finite element method to determine the corresponding numerical eigenfrequencies. After that, an optimisation technique comprised of the minimisation of an error function, which estimates the deviation between experimental and numerical values.

Based on these previous articles, Lopes et al. [8] presented a method for the identification of material constants of laminated composite plates. The optimisation process makes use of an objective function that relates experimental and numerical frequencies to determine the elastic constants of the plate. The algorithms Particle Swarm, Genetic and Pattern Search were used in the optimisation process to estimate the material elastic constants.

2.3. Algorithms for optimisation

A generic optimisation problem can be written in the following way [9]:

Find an n-vector $\mathbf{x} = (x_1, x_2, ..., x_n)$ of design variables to minimise an objective function:

$$f(\mathbf{x}) = f(x_1, x_2, ..., x_n) \quad (2a)$$

subject to the p equality constraints:

$$h_j(\mathbf{x}) = h_j(x_1, x_2, ..., x_n) = 0; j = 1 \quad \text{to} \quad p \quad (2b)$$

and the m inequality constraints:

$$g_i(\mathbf{x}) = g_i(x_1, x_2, ..., x_n) \leq 0; i = 1 \quad \text{to} \quad m \quad (2c)$$

To fully define an optimisation problem it is fundamental to know what are the design variables, the objective function and any constraints that might influence the optimisation solution. One other aspect that has strong influence is the optimisation method. The use of nature-inspired metaheuristic algorithms raises some questions when the complexity and diversity of real-world problems are taken into consideration. Since most algorithms are tested against benchmark functions it is impossible to say that to solve a real-world problem algorithm A is better than algorithm B, as stated by the No-free-lunch Theorem [10].

2.3.1. Description of algorithms

In this section, the algorithms selected are presented and briefly described.

2.3.1.1 Genetic algorithm

The Genetic algorithm (GA) was developed by Holland [11]. In essence, a genetic algorithm is a search method based on the abstraction of Darwinian evolution and natural selection of biological systems [12]. Using biological operators, such as crossover, mutation, and selection of the fittest, to generate the successive generations and evaluate the best values.

2.3.1.2 Particle Swarm Optimisation algorithm

The Particle Swarm Optimisation (PSO) algorithm takes inspiration from the group behaviour of animals, such as swarm intelligence of fishes, birds and even by human behaviour [13]. The multiple search agents called particles, $p_1, .., p_n$, move around the search space starting from an initial random guess. The feasible solutions are called "swarm", $P = \{p_1, ..., p_n\}$. The swarm communicates the current best and shares the global best in order to focus on the best solution found. To solve most of the problems the number of particles used varies from twenty to fifty [10].

2.3.1.3 Grey Wolf Optimisation algorithm

The Grey Wolf Optimisation (GWO) algorithm takes inspiration from the social hierarchy and hunting behaviours of grey wolves as they are apex predators, meaning they are in the top of the food chain with a strict social dominant hierarchy. This social hierarchy is well defined and the grey wolf leaders are denominated as alphas, α. The next level in the hierarchy are the betas, β, followed by the omegas, ω, and the deltas, δ, in the bottom of the pyramid. The hunting behaviour has different stages starting with encircling prey, followed by hunting, attacking prey and search for prey [14].

2.3.1.4 Firefly algorithm

The Firefly algorithm (FA) takes inspiration from the bioluminescence flashes of fireflies. The primary function of these flashes is to attract matting partners and to attract potential prey. The pattern of flashes is specific to each one of the two thousand species of fireflies. The FA was developed and implemented by Yang in 2009 [15]. This algorithm is based on three idealised rules: the first is that all fireflies are unisex, meaning that one firefly will be attracted to the others regardless of their sex; the second one is that the attractiveness is proportional to the brightness and these two factors reduce as the distance between fireflies increase; and the last one is that the less bright firefly will move towards the brighter ones, the fireflies randomly move towards the brightness.

2.3.1.5 Cuckoo Search algorithm

The Cuckoo Search (CS) is inspired by the brood parasitism of some cuckoo species and makes use of the Lévy flights, a behaviour of flight of many birds and insects characterised by straight flights punctuated by sudden 90° turn used to explore new terrain. This algorithm was developed by Yang and Deb in 2010 [16]. The CS can be described by three rules: The first rule is that each cuckoo lays one egg at a time in a randomly chosen nest; the second rule says that the best nest with the high-quality eggs being carried over to the next generations; and the last rule is that the number of host nests is fixed, and there is a probability, $p_a \in [0, 1]$, that the host bird discovers the cuckoo's egg. In this case, the host bird can get rid of the egg or abandon the nest, creating new locations.

3. Methodology

The present method for properties identification is included in the non-direct evaluation methods as it uses a metaheuristic optimisation approach for the identification of material properties.

3.1. Specimens selection

To apply this method, it is fundamental to measure natural frequencies using experimental techniques. Data from previously performed measurements, taking into consideration several aspects regarding boundary conditions, material properties and specimens characteristics, will be used.

To accurately measure natural frequencies, the specimen should be suspended so that it would approximate a free condition. This condition is the one that leads to the best desired measurements. These specimens are rectangular plates with constant thickness. There are a large number of examples in the literature presenting data required to implement this method. However, the selected specimens were chosen as they represent some of the most used materials in composite materials, as well as some green composites. Table 1 lists the selected specimens references, Table 2 lists the specimens materials and their geometric characteristics and Table 3 lists their mechanical properties

Table 1: Specimens references

Specimen	Author	Year	Reference
SP-1	Soares et al.	1993	[6]
SP-2	Lopes et al.	2019	[8]
SP-3	Araújo et al.	1996	[7]
SP-4	Larsson	1997	[17]
SP-5	Igea and Cicirello	2020	[18]

Table 2: Type of material and geometric characteristics of selected specimens

Specimen	Material	a x b x h (mm)	N. of Plies	Fiber Orientation
SP-1	Aluminium	193 x 281 x 1.94	1	–
SP-2	Glass-Epoxy	299.26 x 93.71 x 2.3	14	$[0^0_{14}]_T$)
SP-3	Glass-Epoxy	203 x 136 x 14	-	$[0^0]$
SP-4	OSB*	2440 x 1220 x 10	-	all align
SP-5	Plywood panel	350 x 350 x 5.50	3	all align

*OSB - composite material composed of adhesive and wooden strands.

Table 3: Mechanical properties of selected specimens as reported in the references

Specimens	Density($\mathrm{Kg/m^3}$)	E_1(GPa)	E_2(GPa)	G_{12}(GPa)	G_{13}(GPa)	G_{23}(GPa)	ν_{12}
SP-1	2688	68.7	68.1	24.6	24.6	26.9	0.34
SP-2	1978.3	31.28	27.17	6.46	-	-	0.1659
SP-3	1886.9	42.8	12.2	4.8	4.2	4.9	0.301
SP-4	649.691	7.12	3.45	1.96	-	-	0.28
SP-5	568	8.180	4.357	0.6954	-	-	0.1216

3.2. Mesh convergence study

Since this method relies on FEM analysis, a mesh study is carried out for all the selected specimens. A model for each specimen is created and the simulations required to perform the convergence study are requested in APDL®.

The process to obtain the requested data is as follows: MATLAB® generates an input file which contains ANSYS® script commands. In this file, the specimen plate in question is modelled and a modal analysis is requested to ANSYS®. From the general Equation of motion, the particular case of the free vibration is deduced, assuming all applied loads and the in-plane forces are set to zero:

$$[M]\{\ddot{\Delta}\} + [K]\{\Delta\} = 0 \tag{3}$$

where [M] is the mass matrix, [K] is the stiffness matrix, Δ is the displacement and $\ddot{\Delta}$ is the second-order time derivative of the displacement.

In free vibration analysis the structure's behaviour is assumed to be linear, and the response can be assumed harmonic:

$$\{\Delta\} = \{\phi_i\} cos(\omega_i t) \tag{4}$$

where ϕ_i is the mode shape (eigenvector) and ω_i is the natural circular frequency for mode i. By replacing this last equation in equation (3) yields an eigenvalue problem:

$$([K] - \omega_i^2[M])\{\phi_i\} = 0 \tag{5}$$

which is solved in ANSYS® [19].

For comparison purposes and to avoid distorted elements, the finite element dimensions were defined so that elements are approximately square. The elements used are SHELL63 and element SHELL181.

For the convergence study a convergence index is used to check the mesh and help in the decision of which mesh to use for the rest of the analysis.

$$MCI = 100 \times \frac{\sum_{i=1}^{10} f_{i_{ref}} - \sum_{i=1}^{10} f_i}{\sum_{i=1}^{10} f_{i_{ref}}} \tag{6}$$

where the mesh convergence index (MCI) is related to the sum of the 10 modal frequencies requested, f_i, and the sum of the 10 modal frequencies of a reference mesh with approximately 10000 elements ,$f_{i_{ref}}$.

Table 4 presents the selected meshes that will be used in the upcoming analysis.

Table 4: Number of elements for determined Convergence Index for SHELL63 element-using 10 modal frequencies

Specimen	MCI	# elements	a_e(mm)	a_e/a
SP-1	$MCI < 0.5\%$	176 (11×16)	17,55	0,09091
	$MCI < 0.3\%$	315 (15×21)	12,87	0.0667
SP-2	$MCI < 0.5\%$	252(28×9)	10.69	0.03571
	$MCI < 0.3\%$	1725 (75×23)	3.99	0.0133
SP-3	$MCI < 0.5\%$	54 (9×6)	22.56	0.1111
	$MCI < 0.3\%$	117 (13×9)	15.62	0.07692
SP-4	$MCI < 0.02\%$	392 (28×14)	87,14	0.08714
SP-5	$MCI < 0.02\%$	168 (14×14)	25	0.07143

After analysing the results above, the SHELL63 element graphs convergence was rapid, resulting in the lowest MCI produced from the elements tested. Thus, meshes with MCI $< 0.5\%$ are used from now on, except for specimen SP-2. For this specimen, the mesh used presents an MCI $< 0.3\%$, corresponding to the mesh presented in the article [8] for comparison purposes.

3.3. Optimisation problems

In this section, the optimisation problems are defined. In the present optimisation problems, the design variables are the elastic constants of the different materials.

The optimisation problems defined for the four different specimen material elastic constants can be represented as follows:

Isotropic materials

$$\text{Min } \Phi(E, \nu) \tag{7a}$$

Transversely isotropic materials

$$\text{Min } \Phi(E_1, E_2, G_{12}, \nu_{12}) \tag{7b}$$

Orthotropic materials

$$\text{Min } \Phi(E_1, E_2, G_{12}, \nu_{12}) \tag{7c}$$

Anisotropic materials

$$\text{Min } \Phi(E_1, E_2, G_{12}, G_{13}, G_{23}, \nu_{12}) \tag{7d}$$

The computation of the objective function is represented in the flowchart of Figure 2.

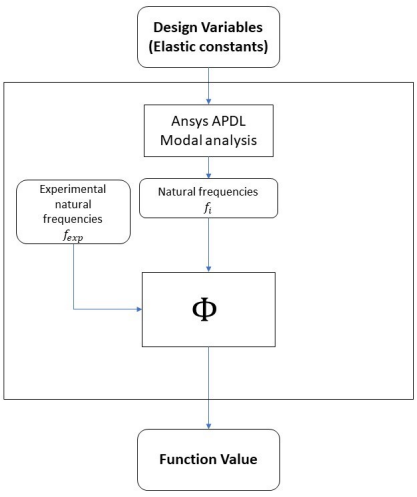

Figure 2: Flowchart of the objective function computation

The first objective function is presented in Equation (8) [8]. The objective is to minimise the sum of the absolute difference between the circular natural frequencies obtained experimentally, $\tilde{\omega_i}$, and the circular natural frequencies obtained computationally, ω_i:

$$\Phi = \sum_{i=1}^{nf} |\tilde{\omega_i} - \omega_i| \tag{8}$$

where nf are the total number of frequencies considered.

One other objective function relates experimental circular natural frequencies, $\tilde{\omega_i}$, and computational circular natural frequencies, ω_i, according to the Equation (9) [6]:

$$\Phi = \sum_{i=1}^{nf} \frac{(\tilde{\omega_i}^2 - C \times \omega_i^2)^2}{\tilde{\omega_i}^4} \tag{9}$$

where $C = \frac{\tilde{\omega_1}^2}{\omega_1^2}$ and nf are the total number of frequencies considered for each of the specimen analysis.

The last step to have a fully defined optimisation problem is to apply the necessary constraints to the design variables. Therefore for each specimen, a set of lower and upper constraints are defined for each one of the design variables. If the reference presents the constraints for the design variables these are used, if not, the constraints are defined accordingly to each specific case. Table 5 lists the constraints for each specimen. The termination criteria are the tolerance and the maximum number of iterations. The tolerance is set to 10^{-6} or 10^{-9} depending on the specimen and objective function. This ensures that the optimisation ends when the relative difference of successive function values reaches this value. The maximum number of iterations is set to one thousand for all optimisation problems. This is needed so that, if the tolerance is not met, the algorithms will stop when they reach the one-thousandth iteration.

Table 5: Constraints applied to each design variable

Specimen	Constraint	E_1(GPa)	E_2(GPa)	G_{12}(GPa)	G_{13}(GPa)	G_{23}(GPa)	ν_{12}
SP-1	Upper	100	-	-	-	-	0.4
	Lower	50	-	-	-	-	0.2
SP-2	Upper	50	50	20	-	-	0.4
	Lower	10	10	1	-	-	0.05
SP-3	Upper	70	25	15	15	15	0.4
	Lower	20	1	1	1	1	0.1
SP-4	Upper	15	10	5	-	-	0.4
	Lower	4	1	0.1	-	-	0.1
SP-5	Upper	15	10	5	-	-	0.2
	Lower	4	1	0.1	-	-	0.05

4. Results and discussion

4.1. Comparison of results obtained with different algorithms

In this section, the optimisations are used to verify the applicability of this method for properties identification. With this aim the specimens SP-1 and SP-2 extracted from [6, 8] are used. For each specimen, optimisations using the five different algorithms proposed are performed. This is done so that the more suitable algorithm can be selected to be used in the next sections. The optimisation problems analysed in this section are summarised in Table 6 and the constraints applied to the design variables listed in Table 5.

Table 6: Optimisation problems' parameters

Specimen	SP-1	SP-2
Parameter	Value	Value
Objective function	Equation (9)	Equation (8)
nf	9	14
Number of search agents	100	100
Tolerance	10^{-9}	10^{-6}
Max. number of iterations	1000	1000

4.1.1. Specimen SP-1

For SP-1, the design variables are E and ν ,and it is expected to obtain values similar to the ones reported in [6].

The elastic constants computed and the relative difference to the reference values [6] calculated are shown in Table 7. All the algorithms have the same values for the Poisson's ratio, ν. Only for Young's modulus, E, is it possible to draw any conclusions. In this set of optimisations, this design variable presents

distinct values for each of the algorithms. Table 8 lists the function values (Fval), the number of iterations (Niter), the number of function evaluations (NFEs), and the relative computational time (RCTime) taken by each algorithm.

Table 7: Elastic constants computed with each of the algorithm and relative difference for SP-1

	E (GPa)	ν	$100 * \frac{\lvert E-E_{ref}\rvert}{E}$	$100 * \frac{\lvert \nu-\nu_{ref}\rvert}{\nu}$
Reference [6]	68.7	0.34	-	-
GA	71.09	0.37	3.4	7.9
PSO	69.14	0.37	0.6	7.9
GWO	87.41	0.37	21.4	7.9
FA	78.68	0.37	12.7	7.9
CS	99.62	0.37	31.0	7.9

Table 8: Function values (Fval), number of iterations (Niter), number of function evaluations (NFEs) and relative computational time (RCTime) for each algorithm for SP-1

	Fval	Niter	NFEs	RCTime
GA	0.001041	65	6600	1.72
PSO	0.001041	35	3600	1.00
GWO	0.001041	996	99700	54.76
FA	0.001041	82	8200	2.65
CS	0.001041	118	11800	1.04

Analysing Table 7 the best result is obtained for the PSO algorithm, presenting a relative error of zero point six per cent. All other algorithms present relative differences above ten per cent, making them unsuitable for solving this kind of problems.

In conclusion, to solve this optimisation problem the most suitable algorithm is the PSO, which manages to obtain values for the design variables close to the reference values while using fewer iterations and time when compared to all others algorithms used.

4.1.2. Specimen SP-2

For SP-2, the design variables are E_1, E_2, G_{12} and ν_{12}.

The elastic constants computed using each algorithm for this specimen are listed in Table 9. The elastic constants computed using the different algorithms are in the vicinity of the reference values.

From Table 10, it is observed that the GWO and the FA algorithms have the greatest differences. The relative differences observed in all algorithms are due to the type of element used. Although the same number of elements is being used, the finite element used is different from the one used in reference [8]. In this article, the Kirchoff non-conforming element of four nodes and three degrees of freedom per node was used, while in this method, the shell element SHELL63 is used.

Table 9: Elastic constants computed with each of the algorithms for SP-2

	E_1(GPa)	E_2(GPa)	G_{12}(GPa)	ν_{12}
Reference [8]	31.28	27.17	6.46	0.1659
GA	30.57	27.16	6.38	0.1609
PSO	30.51	27.15	6.38	0.1673
GWO	30.98	27.34	6.50	0.0885
FA	27.17	30.59	6.4	0.1579
CS	30.51	27.15	6.38	0.1676

Table 10: Relative difference of computed elastic constants of each algorithm

	$100 * \frac{\lvert E_1-E_{1_{ref}}\rvert}{E_1}$	$100 * \frac{\lvert E_2-E_{2_{ref}}\rvert}{E_2}$	$100 * \frac{\lvert G_{12}-G_{12_{ref}}\rvert}{G_{12}}$	$100 * \frac{\lvert \nu_{12}-\nu_{12_{ref}}\rvert}{\nu_{12}}$
GA	2.32	0.037	1.25	3.11
PSO	2.52	0.074	1.25	0.84
GWO	0.97	0.62	0.61	87.46
FA	15.13	11.18	0.94	5.07
CS	2.52	0.074	1.25	1.01

Analysing Table 11, it is possible to see that the function values for most of the algorithms do not vary much. However, for the GWO algorithm, the function value obtained is around three times greater than any other. The algorithm that took the longest was the FA, taking almost eight times more than the fastest one, the GA.

After analysing both of these sets of optimisations, it is possible to see that the most efficient algorithms are the GA and the PSO. For both specimens, these algorithms are the ones that present the most relevant results, with the lowest amount of time and iteration spent to obtain it.

Table 11: Function values (Fval), number of iterations (Niter), number of function evaluations (NFEs) and relative computational time (RCTime) for each algorithm for SP-2

	Fval	Niter	NFEs	RCTime
GA	47.76	145	14600	1.00
PSO	45.66	101	10100	1.08
GWO	148.87	1000	100000	3.41
FA	48.70	916	91600	7.73
CS	45.75	622	31100	4.51

4.1.2.1 Comparison of results with different sets of experimental natural frequencies

In this analysis the algorithm used is the PSO algorithm for both cases. The presented method is applied to the modelled plate of this specimen, changing the input experimental frequencies for each case. Since in the more recent measurements of the natural frequencies, only ten frequencies were measured. In the present analyses, the number of frequencies used, nf, is set to ten for both cases. The set of natural frequencies presented in the article [8] is denoted as $\tilde{f}i_{a)}$ and the more recent set is denoted as $\tilde{f}i_{b)}$.

Table 12 lists the elastic constants computed for each case and the best function value obtained in the optimisation process.

Table 12: Elastic constants and function value obtained for each one of the cases a) and b)

	E_1(GPa)	E_2(GPa)	G_{12}(GPa)	ν_{12}	Fval
a)	30.61	27.18	6.41	0.1555	10.21
b)	30.14	27.74	6.08	0.2000	19.15

Here it can be observed that for the Young's moduli, E_1 and E_2, the values obtained are very similar and within the acceptable values for this constant. This is also observed for the shear modulus. The Poisson's ratio is the elastic constant that presents the most significant variation, presenting a relative difference of around twenty per cent from the reference [8], for case b).

All things considered, the elastic constants computed with each set of experimental frequencies present similar values, except for the Poisson's ratio, which is proven to be more sensitive to the changes in frequency than the other elastic constants. The high sensitivity of the Poisson's ratio was also verified in [7] .

4.2. Comparison of results obtained with different sets of search agents

The present method is based on meta-heuristics, so there is a need to validate this method. For that, in this section, one of the most used validation tests discussed in [20] is going to be performed.

In this section, fifty optimisations are performed for SP-1 and thirty optimisations for SP-2. The optimisation problems analysed in this section are summarised in Table 13 and the constraints applied to the design variables listed in Table 5.

Table 13: Optimisation problems' parameters

Specimen	SP-1	SP-2
Parameter	Value	Value
Objective function	Equation (8)	Equation (8)
nf	9	14
Number of search agents	50	100
Tolerance	10^{-6}	10^{-9}
Max. number of iterations	1000	1000

The computer used for this analysis has an Intel® Core™ i7-9750H CPU @2.60 GHz processor with 16 GB of RAM. It was also used the software AMD® Radeon™ RAMDISK which allows allocating part of the computers RAM memory into a virtual disc.

4.2.1. SP-1

The next set of fifty optimisations are performed for the specimen SP-1.

After gathering the necessary data from all the fifty optimisations the averages and standard deviations of all the design variables, the objective function value and computational time are calculated and displayed in Table 14.

The average values obtained for both elastic constants, E and ν, are close to the values showcased in the reference [6]. For the standard deviations, it presents values with a magnitude of 10^{-14} for E, and 10^{-16} for ν which demonstrates the reliability of this method determining the material elastic constants of the material.

Table 14: Average and standard deviation of fifty optimisation runs for the elastic constants, function value and computational time

	E (GPa)	ν	Fval	Computational time (h)
Average	66.8	0.38	72.75	1.052
Standard deviation	0.0000	0.0000	0.0000	0.1049

The objective function values presented in all the optimisations have approximately the same value and showcasing a standard deviation with magnitude of 10^{-14}. To examine in detail the influence of each of the initial populations of search agents the computational time is studied. The best-case scenario took approximately zero point eighty-four hours, and the worst-case scenario which took approximately one point thirty three hours. The time difference between the best and the worst-case is around zero point forty-nine hours, corresponding to approximately thirty minutes. Both optimisations used different numbers of iterations, the worst-case used seventy-two iterations, and the best case used forty-six iterations. To analyse each case, the dispersion of the search agents throughout the optimisation process are represented in Figure 3.

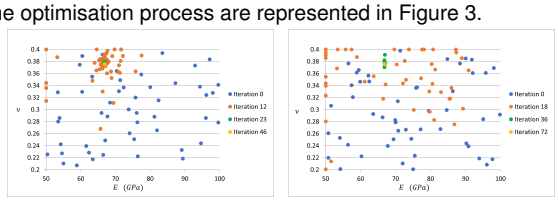

(a) Best case **(b)** Worst case

Figure 3: Dispersion of the design variable throughout the optimisation process for the best and the worst case

The iterations represented in the figures correspond to the initial iteration, followed by the iteration corresponding to the one-quarter of the optimisation process, the next corresponds to half of the optimisation process and finally, the last iteration of the optimisations. For both cases, the initial population seems to explore the search space evenly, with the worst case population grouped into small swarms through the search space whereas the best case population is more scattered through the search space.

The extreme cases are computed as well making the initial population agents placed at the upper bounds and the lower bounds for the design variables. In these extreme cases, it is possible to denote that even with the initial populations at the constraints bounds, this method is capable of obtaining the correct elastic constants, without major variances in computational time and iterations.

4.2.2. SP-2

In this section, the optimisations are performed for specimen SP-2.

The elastic constants computed in each run, as well as the objective function value and computational time, are gathered from the performed optimisation. Table 15 lists the averages and standard deviations of these parameters. As it happened in the subsection 4.2.1, the elastic constants average values are very close to the values produced in the reference [8] and with reduced standard deviations. In this case, the shear modulus, G_{12}, and the Young's modulus E_1 showcase standard deviations with the same order of magnitude. The Young's modulus E_2 and the Poisson's ratio, ν_{12}, present standard deviations with the same order of magnitude smaller than for the other two design variables with a magnitude of 10^{-5}. The function value presents a small variation proving that despite the different initial populations, the global function minimum is determined with some certainty.

Table 15: Average and standard deviation of thirty optimisation runs for the elastic constants, function value and computational time for SP-2

	E_1 (GPa)	E_2 (GPa)	G_{12} (GPa)	ν_{12}	Fval	Computational time (h)
Average	30.51	27.15	6.38	0.1673	45.66	11.15
Standard deviation	0.0020	1.534E-05	0.0067	6.187E-05	0.0112	3.702

The effect of the different initial population is more noticeable in the computation time each optimisation took than in these last parameters. The computation time presents an average of around eleven hours and a standard deviation of around three point seven hours, which is significant corresponding to almost one-third of the average computational time. The high standard deviation of the computation time is noticeable with the computational time varying from around six hours to as much as twenty hours.

In the best-case scenario, the PSO algorithm performed the optimisation process in a bit more of six hours using one hundred and thirty-four iterations. For the worst case, the PSO used more than twenty hours performing three hundred and seventy-four iteration.

In the next figure, Figure 4, are represented the evolution of the best values for the design variables in each iteration.

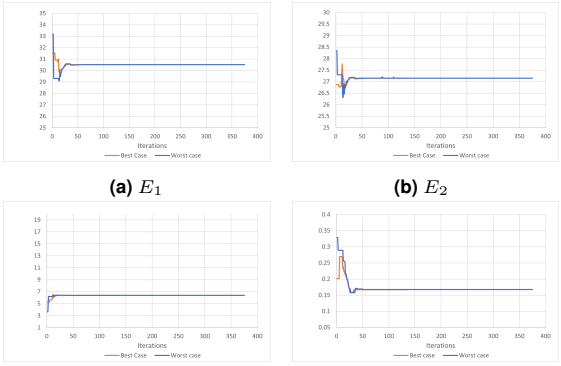

(a) E_1 **(b)** E_2

(c) G_{12} **(d)** ν_{12}

Figure 4: Evolution of the design variables (E_1, E_2, G_{12} and ν_{12}) values throughout iterations for both the best and worst case

For the graphs from Figure 4, it is visible that the worst case scenario has a broader exploration of the search space. This stands out in the v_{12} graph, where the search particles cover more than half of the search space before stabilising in the final value. While for the best case graphs from Figure 4, all the initial elastic constants are within a close range of the final value achieving this value around the fortieth iteration.

These specific optimisations, best case scenario and worst case scenario together with the data gathered from the thirty other optimisations demonstrate that the time each optimisation uses may vary from the different set of search agent. Despite that, the validity of this method for properties identification is verified regardless of the initial set of search agents.

With the data from these two studies using SP-1 and SP-2, it was possible to demonstrate the independence to achieve the correct elastic constants independently of the initial population of search agents.

4.3. Comparison of results obtained with different objective functions

In this section, the objective is to study the influence of the objective function used. The optimisations are performed using the PSO algorithm, changing only the objective function. In this set of optimisations the specimen used is the SP-2, the constraints applied to the design variables are listed in Table

5. These optimisation problems are defined in Table 13 using different objective functions.

The objective functions used in this analysis are the ones used in section 4.1, Equation (8), Φ_1, and (9), Φ_2, and a new objective function, Φ_3 [21]:

$$\Phi_3 = \sum_{i=1}^{nf} (fr_i - \tilde{fr_i})^2 \tag{10}$$

where fr_i and $\tilde{fr_i}$ are the computational and experimental frequencies, respectively, and nf the number of frequencies considered for each analysis.

These objective functions were created in order to solve or overtake problems presented in other types of property identification methods. This is implemented either to escape second derivatives, which can be challenging to compute, for example, Φ_1, or to deal with gradient-based methods. Functions like Φ_2 and Φ_3 are known as the sum of squares and were developed to be used by gradient-based methods. Since the present method is a gradient-free method, the objective function used should have a small influence on the method. The values obtained for the design variables, the computational time, the number of iterations each optimisation took, and the final objective function value obtained for each one of the objective functions are presented in Table 16.

Table 16: Elastic constants computed, relative computational time (RCTime), number of iterations (Niter) and function values (Fval) obtained for SP-2 using different objective functions

Objective function	E_1(GPa)	E_2(GPa)	G_{12}(GPa)	ν_{12}	RCTime	Niter	Fval
Φ_1	30.51	27.15	6.38	0.1674	2.10	101	45.65960
Φ_2	49.99	44.48	10.53	0.1699	1.00	57	0.000068
Φ_3	30.48	27.16	6.38	0.1656	2.11	107	6.145190
Reference [8]	31.28	27.17	6.46	0.1659	-	-	-

The objective functions Φ_1 and Φ_3 obtained the best results for the computed elastic constants. The elastic constant computed with these two functions are similar and closer to the reference values than the ones obtained using Φ_2. Thus Φ_2 does not seem to be suited to solve this optimisation problem when compared to the other objective function analysed. When comparing the Φ_1 and Φ_3 values, the difference between the values obtained are minimal, and the most significant difference is in the function values.

Φ_1 uses slightly less time than Φ_3, therefore Φ_1 is more suitable to be used to solve this type of optimisation problems.

4.4. Influence of the number of natural frequencies

In this section, the objective is to analyse the influence of the number of natural frequencies in the optimisation using the PSO algorithm. The optimisations problems used are defined in Table 17 and the constraints for the different design variables are presented in Table 5.

Table 17: Optimisation problems' parameters

Specimen	SP-1	SP-2	SP-3
Parameter	Value	Value	Value
Objective function	Equation (8)	Equation (8)	Equation (8)
nf	9	14	12
Number of search agents	50	50	100
Tolerance	10^{-6}	10^{-6}	10^{-6}
Max. number of iterations	1000	1000	1000

4.4.1. SP-1

For SP-1 [6], two design variables are considered.

In Table 18 the elastic constants computed using the different number of frequencies, the average, the standard deviation of the design variables, and the reference values are presented. The design variables have a small deviation for the different number of frequencies. The average design variables values obtained for this set of optimisations have a relative error to the reference values of around two per cent.

For this specimen, nine frequencies are used. However, with the analysis of the Table 18, the optimisation that came closer to the reference value of this specimen are the one that uses five frequencies.

Table 18: Elastic constants computed, average and standard deviation while using PSO for each number of frequencies for SP-1

nf	E(GPa)	ν
1	68.1	0.40
2	67.9	0.39
3	67.2	0.40
4	66.7	0.38
5	67.0	0.37
6	67.5	0.34
7	66.4	0.36
8	66.4	0.36
9	66.8	0.38
Average	67.1	0.37
Standard Deviation	0.5655	0.0194
Reference [6]	68.7	0.34

4.4.2. SP-2

For these optimisation problems four design variables were used, and the number of frequencies is the variable analysed. Table 19 lists the elastic constants computed for each number of frequencies used in the optimisation process. This table also presents the average and the standard deviation of each one of the design variables.

The highest deviation observed for the E_1 is presented in the optimisations with four and five frequencies. The values for this design variable are approximately half of what is expected to be obtained.

Table 19: Elastic constants computed and its average and standard deviation, while using PSO for each number of frequencies for SP-2

nf	E_1(GPa)	E_2(GPa)	G_{12}(GPa)	ν_{12}
1	33.42	26.95	8.08	0.3422
2	33.08	27.10	6.44	0.1380
3	41.16	27.04	6.43	0.3005
4	13.48	27.03	6.46	0.1328
5	14.49	27.04	6.45	0.1388
6	25.83	27.09	6.41	0.1728
7	38.90	27.20	6.39	0.1696
8	28.82	27.11	6.40	0.1805
9	30.61	27.18	6.41	0.1550
10	30.61	27.17	6.41	0.1559
11	30.67	27.17	6.42	0.1464
12	30.60	27.15	6.41	0.1566
13	30.48	27.12	6.40	0.1705
14	30.51	27.15	6.40	0.1672
Average	29.48	27.11	6.54	0.1805
Standard Deviation	7.346	0.06847	0.4293	0.05964
Reference [8]	31.28	27.17	6.46	0.1659

The design variables computed using fourteen frequencies presents values are in good agreement to the reference[8]. However, with less frequencies similar results can be obtained namely with nine frequencies.

The abnormal results for three, four and five frequencies, might have been the result of less accurate measurements during the experimental modal analysis. These less accurate measurements might also have been caused by the poor-quality signal captured by the laser vibrometer described in [8].

When comparing both these sets of optimisations, it is possible to observe that for the SP-2, a higher dispersion of the elastic constants is presented than for the SP-1. However, the complexity of each case is very different. The SP-1 only has two design variables, in comparison to the SP-2 that has four design variables, making it a much more complex problem to solve.

4.4.3. SP-2 with weight factor

In this subsection, a new objective function is formulated based on Equation (8) to improve the results of this last set of optimisations and to better understand the influence of the number of frequencies and modes used. This new objective function is represented as the weighted difference of frequencies for each number of frequencies used.

$$\Phi = \sum_{i=1}^{nf} W_i \times |\tilde{\omega_i} - \omega_i| \tag{11}$$

where $\tilde{\omega_i}$ and ω_i are experimentally and computationally obtained circular frequencies, respectively. W_i is the weight factor, and nf are the total number of frequencies considered.

The weight factor in this first approach is set as zero or one. To define this factor, the relative differences between each experimentally determined frequencies, from [8], and computationally determined ones, from the optimisation using $nf = 14$ from subsection 4.4.2, are calculated. If this relative difference exceeds five percent the weight factor is set as zero otherwise it is set as one.

The modes that exceed the threshold are the first, the third, the eighth, the ninth, and the thirteenth frequencies, and so the weight factor for these modes are set to zero. Therefore the maximum effective number of frequencies used in this set of optimisations is nine. Table 20 exhibits the effective number of frequencies used, the elastic constants computed, and the weight factor vector considered for each case. This set of elastic constants presents an higher variation with the increase of the effective number of frequencies, for all constants when compared to the set obtained in Subsection 4.4.2.

Table 20: Effective number of frequencies considered, elastic constants computed and weight factor vector for Equation (11), for each number of frequencies for SP-2

Effective nf	E_1(GPa)	E_2(GPa)	G_{12}(GPa)	ν_{12}	Weight factor vector
1	14.28	46.45	6.31	0.1204	[0,1]
2	44.12	24.26	6.45	0.3551	[0,1,0,1]
3	32.57	26.62	6.35	0.3535	[0,1,0,1,1]
4	50.00	10.24	20.00	0.4000	[0,1,0,1,1,1]
5	47.71	27.25	6.38	0.1570	[0,1,0,1,1,1,1]
6	30.81	27.22	6.44	0.1304	[0,1,0,1,1,1,1,0,0,1]
7	30.29	27.05	6.44	0.1304	[0,1,0,1,1,1,1,0,0,1,1]
8	30.29	27.05	6.39	0.1888	[0,1,0,1,1,1,1,0,0,1,1,1]
9	30.69	27.20	6.42	0.1414	[0,1,0,1,1,1,1,0,0,1,1,1,0,1]
Average	34.67	28.57	7.44	0.2055	-
Standard Deviation	11.63	8.83	3.63	0.0931	-
Reference [8]	31.28	27.17	6.46	0.1659	-

With the increase of the number of frequencies used, the elastic constants computed get close to the values presented in the reference article [8]. With eight and nine frequencies used, the values computed for the elastic constants are similar to the reference.

To better understand the influence of the frequencies used and the number needed to determine the elastic constants accurately, the elastic constants computed using nf equal fourteen from Table 19 and the elastic constants computed for nf equals nine are compared in Table 21.

Table 21: Comparison of the computed elastic constants for nf equals fourteen and for effective nf equals nine

Effective nf		E_1(GPa)	E_2(GPa)	G_{12}(GPa)	ν_{12}
-	Reference [8]	31.28	27.17	6.46	0.1659
14	Computational	30.51	27.15	6.40	0.1672
	Average	29.48	27.11	6.54	0.1805
	Computational relative difference (%)	2.462	0.07361	0.9288	0.7836
	Average relative difference (%)	5.766	0.2343	1.181	8.798
9	Computational	30.69	27.20	6.42	0.1414
	Average	34.53	27.04	6.42	0.2197
	Computational relative difference (%)	1.886	0.1104	0.6192	14.77
	Average relative difference (%)	10.84	5.135	15.10	23.85

Comparing the average values and its relative differences between both cases, it is observed that the case with $nf = 9$ displays greater relative differences when compared to the case with $nf = 14$. Despite that, the optimisation with effective $nf = 9$ presents better results for Young's modulus E_1 and for the shear modulus G_{12} than the optimisation which uses all fourteen frequencies. The Young's modulus E_2 obtained with $nf = 14$ displays a relative difference smaller than for the shear modulus computed in the other optimisation. For the Poisson's ratio ν_{12}, the same behaviour is displayed. However, in this case, the difference is more significant. With $nf = 14$, the relative difference displayed is around zero point eight per cent, whereas in this case, with $nf = 9$, the relative difference is around fifteen per cent. This behaviour the Poisson's ratio was already studied by Frederiksen which carried out a sensitivity analysis of the Poisson's ratio.

With this new proposed objective function, the elastic constants computed are within the acceptable range except for the Poisson's ratio, which demonstrates being more sensitive to natural frequencies used to estimate this elastic constant.

4.4.4. SP-3

For SP-3, the optimisation problem presents six design variables.

With the optimisation problem fully defined, the optimisations can be solved. The number of frequencies used, the elastic constants computed are listed in Table 22.

Table 22: Computed elastic constants and its average and standard deviation while using PSO for each number of frequencies for SP-3

nf	E_1(GPa)	E_2(GPa)	G_{12}(GPa)	G_{13}(GPa)	G_{23}(GPa)	ν_{12}
1	57.8	3.6	7.9	8.6	6.4	0.275
2	39.3	19.1	4.2	7.7	9.5	0.149
3	58.6	7.8	4.3	10.0	5.9	0.159
4	49.0	9.8	3.9	3.9	1.7	0.100
5	49.7	9.4	3.7	8.6	9.1	0.244
6	49.0	9.8	3.6	6.0	11.9	0.100
7	58.7	6.4	4.0	4.1	8.9	0.157
8	44.7	8.8	4.4	1.6	4.0	0.312
9	40.7	7.9	4.7	12.6	8.9	0.251
10	35.7	15.2	2.9	9.1	11.7	0.100
11	50.6	6.0	4.6	7.9	6.3	0.225
12	49.5	6.4	4.8	5.2	10.3	0.100
Average	48.6	9.2	4.4	7.1	7.9	0.181
S. Deviation	7.2	4.0	1.2	2.9	2.9	0.074
Reference [7]	42.8	12.2	4.8	4.2	4.9	0.301

As the number of design variables increases, so does the complexity of these optimisations increases as well. The results obtained in this set of optimisations are further from the reference than in the first two sets of optimisations with fewer design variables.

In this case, analysing the average values for the design variables some discrepancies are found. Namely for the transverse shear moduli, G_{13} and G_{23}, and for the Poisson's ratio, ν_{12}. The discrepancies in the G_{13} and G_{23} are mainly because transverse shear deformations are only noticed for thick plates. As these plates are relatively thin, these moduli have low sensitivity. The discrepancies in the ν_{12} can be explained by the small sensitivity when compared to other in-plane elastic constants. This is more pronounced for anisotropic plates, which is the case of this plate [7].

From the number of frequencies used, a rule of thumb can be verified by the first specimen that uses two design variables and needs at least four frequencies, by the second specimen that uses four design variables and needs at least eight frequencies. The last specimen, which uses six design variables needs at least twelve frequencies to obtain valid results. This means that twice as many frequencies are needed than the number of design variables.

4.5. Comparison of results with different number of search agents

In this section is studied the influence of the number of search agents for the PSO algorithm. For this analysis the specimen used is SP-2 and the number of search agents is incremented, starting with ten agents, increasing ten agents each time until it reaches a hundred search agents. Table 23 summarises this optimisation problem and the constraints for this specimen design variables are listed in Table 5.

Table 23: Optimisation problem's parameters

Parameter	Value
Objective function	Equation (8)
nf	14
Tolerance	10^{-6}
Max. number of iterations	1000

Table 24 lists the elastic constants computed using the different number of search agents, the function values and the relative time for the PSO algorithm.

It is possible to observe that as the number of search agents increases, the function values decrease, tending to around forty-five.

From Table 24, it is possible to observe that as the number of search agents increases, the differences between the computed values and the results from[8] decrease, staying approximately constant for more than fifty agents.

Table 24: Elastic constants computed, function values (Fval) and relative computational time (RCTime) for different numbers of search agents for PSO algorithm

Number of search agents	E_1(GPa)	E_2(GPa)	G_{12}(GPa)	ν_{12}	Fval	RCTime
Reference [8]	31.28	27.17	6.46	0.1659	-	-
10	37.40	10.00	20.00	0.0500	2099.55	1.00
20	37.40	10.11	20.00	0.0500	2070.54	2.75
30	30.51	27.15	6.38	0.1673	45.67	17.05
40	37.40	10.11	19.73	0.0500	2039.11	4.42
50	30.51	27.15	6.40	0.1672	45.69	11.81
60	30.51	27.15	6.40	0.1672	45.68	11.92
70	30.51	27.15	6.37	0.1674	45.65	22.24
80	30.51	27.15	6.40	0.1672	45.69	22.43
90	30.51	27.15	6.38	0.1673	45.67	17.18
100	30.51	27.15	6.38	0.1673	45.65	17.50

The number of search agents that present the best results are thirty search agents and for more than fifty search agents. These search agents present the lowest function values and the lowest relative differences.

In view of the above results, the PSO algorithm should be used with fifty search agents.

4.6. Green composites

In this section, the objective is to verify the applicability of this method to green composites and wood specimens.

The two specimens of green composites are one of wooden strands bonded with adhesive and another of plywood of birch panels are studied. The specimens were studied by Larsson [17] and by Igea and Cicirello [18], by using respectively a dynamic test based on modal analysis and calculated numerical eigenvalues [17]; and numerical optimisation for the estimation of elastic constants using experimental data from the Chladni patterns and experimental modal analysis [18]. The optimisation problems analysed in this section are summarised in Table 25 and the design variable constraints are displayed in Table 5.

Table 25: Optimisation problems' parameters

Specimen	SP-4	SP-5
Parameter	Value	Value
Objective function	Equation (8)	Equation (8)
nf	7	5
Number of search agents	50	50
Tolerance	10^{-6}	10^{-6}
Max. number of iterations	1000	1000

4.6.1. Specimen SP-4 using objective function Equation (8)

For SP-4 [17], the optimisation problem presents four design variables, which are E_1, E_2, G_{12}, and ν_{12}.

Table 26 lists the elastic constants computed with each one of the optimisation algorithms, and Table 27 lists the relative differences of each one of the computed elastic constants.

Table 26: Elastic constants computed with each of the algorithm for SP-4 using objective function in Eq. (8)

	E_1(GPa)	E_2(GPa)	G_{12}(GPa)	ν_{12}
Reference [17]	7.12	3.45	1.96	0.28
GA	7.42	2.47	2.98	0.35
PSO	7.40	2.45	2.97	0.38
GWO	7.42	2.47	2.98	0.34
FA	7.46	2.51	2.99	0.27
CS	7.39	2.44	2.97	0.40

Table 27: Relative difference of computed elastic constants of each algorithm using objective Function Eq. (8) for SP-4

	$100 * \frac{\lvert E_1 - E_{1_{ref}} \rvert}{E_1}$	$100 * \frac{\lvert E_2 - E_{2_{ref}} \rvert}{E_2}$	$100 * \frac{\lvert G_{12} - G_{12_{ref}} \rvert}{G_{12}}$	$100 * \frac{\lvert \nu_{12} - \nu_{12_{ref}} \rvert}{\nu_{12}}$
GA	4.05	39.96	34.22	19.77
PSO	3.78	40.91	34.04	26.63
GWO	4.09	39.87	34.25	18.72
FA	4.51	37.64	34.42	3.81
CS	3.63	41.47	33.95	29.88

The Young's modulus, E_1, is the elastic constant that presents the closest values to the reference one across all algorithms, presenting a relative difference of around four per cent. The E_2 presents a much higher relative difference around forty per cent, performing all algorithms similarly. For the shear modulus, G_{12}, the optimisation presents values lower than the reference value, with a relative difference of around thirty-four per cent. The FA algorithms stands out when looking to Poisson's ratio, presenting a closer value to the reference among all the algorithms, presenting the lower difference only around four per cent.

Table 28 presents the function value, the number of iterations, the number of function evaluations and the relative computational time obtained for each algorithm. All the algorithms reach around the same value for the function value. However, the GWO used one thousand iterations, reaching the maximum number of iterations allowed. The algorithm that took the least iterations was the PSO, needing only ninety-eight iterations. The one that took the longest time was the GWO with five hundred thousand objective function evaluations.

Table 28: Function values (Fval), number of iterations (Niter), number of function evaluations (NFEs) and relative computational time (RCTime) for each algorithm for SP-4 using objective function in Eq. (8)

	Fval	Niter	NFEs	RCTime
GA	120.31	111	5600	1
PSO	120.25	98	4950	1.07
GWO	120.32	1000	50000	12.94
FA	120.87	344	17200	3.65
CS	120.22	644	32200	8.97

For this specimen, this method was able to estimate the elastic constants within acceptable accuracy. However, if more frequencies were presented in the reference [17], a better estimate could be obtained. According to the thumb rule, at least twice as many frequencies are needed as the number of elastic constants, so at least eight natural frequencies would be needed. From this set of optimisations, the algorithm that had the best values computed for the design variables is the FA. Showing that depending on the optimisation problem, the most suited algorithm to be used with this method can change.

4.6.2. Specimen SP-5 using objective function Equation (8)

For SP-5 [18], the optimisation problem has four design variables, which are E_1, E_2, G_{12}, and ν_{12}.

Table 29 lists the computed elastic constants and Table 30 lists the relative differences of the elastic constants computed with the reference from [18].

Table 29: Elastic constants computed with each of the algorithm for SP-5 using objective function Eq. (8)

	E_1(GPa)	E_2(GPa)	G_{12}(GPa)	ν_{12}
Reference [18]	8.180	4.357	0.6954	0.1216
GA	7.388	4.507	0.7288	0.1805
PSO	7.271	4.537	0.7168	0.2000
GWO	7.256	4.537	0.717	0.2000
FA	7.896	4.399	0.736	0.0878
CS	7.271	4.537	0.7168	0.2000

The elastic constants present approximately the same values for the E_1. However, the values obtained for ν_{12}, in the PSO, the GWO, and the CS correspond to the upper bound of the constraints applied to this design variable. The largest relative differences are observed in these cases. The lowest values for the relative differences are presented for the GA algorithm, followed next for the FA algorithm.

Table 30: Relative difference of computed elastic constants of each algorithm using objective Function Eq. (8) for SP-5

	$100 * \frac{\lvert E_1 - E_{1_{ref}} \rvert}{E_1}$	$100 * \frac{\lvert E_2 - E_{2_{ref}} \rvert}{E_2}$	$100 * \frac{\lvert G_{12} - G_{12_{ref}} \rvert}{G_{12}}$	$100 * \frac{\lvert \nu_{12} - \nu_{12_{ref}} \rvert}{\nu_{12}}$
GA	10.72	3.32	4.59	32.63
PSO	12.51	3.96	2.99	39.20
GWO	3.98	12.74	2.98	39.20
FA	0.95	3.60	5.49	38.47
CS	12.51	3.96	2.99	39.20

Table 31: Function values (Fval), number of iterations (Niter), number of function evaluations (NFEs) and relative computational time (RCTime) for each algorithm for SP-5 using Objective Function Eq. (8)

	Fval	Niter	NFEs	RCTime
GA	142.04	196	9850	8.37
PSO	136.20	82	4150	1.00
GWO	136.41	1000	50000	18.52
FA	176.77	1000	50000	17.87
CS	136.20	968	48400	15.90

In Table 31, the function values, number of iterations, number of function evaluations, and relative computational time for each of the optimisations are listed, using the different algorithms. The PSO and the CS present the lowest function value. However, these algorithms present the most significant relative difference when comparing to the reference. The GWO and the FA algorithms reach the maximum number of iterations, thus not meeting the desired tolerance as a termination criterion. Despite that, the FA algorithm is the one that obtained better results for the E_1 and E_2.

For this specimen, the presented method did not achieve the desired results, mainly due to the low number of frequencies presented in the reference article [18]. For the presented method, at least eight natural frequencies are needed. Nevertheless, the GA algorithm was able to obtain elastic constants with the lowest overall differences.

5. Conclusions

In this work, the main achievement was the development of a computational method for material proprieties identification in composite structures using commercial software, which was achieved. The presented method uses a derivative-free approach based on metaheuristic algorithms.

This method presents several advantages in comparison to other methods for material properties identification. One of the major advantages of this method is that it does not require an initial guess of the elastic constants to be computed, only requiring that the upper and lower constraints for the elastic constants are correctly defined. One other advantage is not requiring the determination of gradients to evaluate the objective function. Another advantage is that it can be easily adapted to obtain the desired elastic constants of different materials and different construction methods not requiring an extensive study of the numerical methods to estimate the material elastic constants accurately.

The most significant disadvantage is the computation time needed to generate the necessary data required so that the algorithm can evaluate the objective function and determine the function minimum, while other numerical and analytical methods require less time to estimate the elastic constants of the materials.

In a nutshell, this method has proven to be precise in computing the elastic constants of the specimens studied, as long as that enough experimental natural frequencies are provided.

The future work includes optimisation of the search algorithm used in order to reduce the computational time even more. However, not excluding the search for more efficient metaheuristic nature-inspired optimisation algorithms or any other non-derivative optimisation methods.

For further studies, it would be interesting to have more sets of experimental natural frequencies of the same specimen to be able to, in more detail, analyse the influence of the differences in the measure of these frequencies. As well as search for more specimens with other material and geometric characteristics to apply this method. Exploring new green composites materials like the emerging flax fibres reinforced composites.

References

[1] S. M. Almufti. Historical survey on metaheuristics algorithms. *International Journal of Scientific World*, 7(1):1, 2019. doi: 10.14419/ijsw.v7i1.29497.

[2] I. Fister, X. S. Yang, J. Brest, and D. Fister. A brief review of nature-inspired algorithms for optimization. *Elektrotehniski Vestnik/Electrotechnical Review*, 80(3):116–122, 2013.

[3] R. Rivello. *Theory and Analysis of Flight Structures*. McGraw-Hill series in aeronautical and aerospace engineering. McGraw-Hill, 1969. ISBN: 9780070529854.

[4] J. N. Reddy. *Mechanics of Laminated Composite Plates and Shells: Theory and Analysis, Second Edition*. CRC Press, 2 edition, 2003. ISBN: 9780849315923.

[5] J. H. Tam, Z. C. Ong, Z. Ismail, B. C. A. , and S. Y. Khoo. Identification of material properties of composite materials using nondestructive vibrational evaluation approaches: A review. *Mechanics of Advanced Materials and Structures*, 24(12):971–986, 2017. doi: 10.1080/15376494.2016.1196798.

[6] C. M. M. Soares, M. M. de Freitas, A. L. Araújo, and P. Pedersen. Identification of material properties of composite plate specimens. *Composite Structures*, 17:971–978, 1993. doi: 10.1016/0263-8223(93)90174-O.

[7] A. L. Araújo, C. M. Soares, and M. M. de Freitas. Characterization of material parameters of composite plate specimens using optimization and experiemental vibrational data. *Composites*, Part B(27B):185–191, 1996. doi: 10.1016/1359-8368(95)00050-X.

[8] H. Lopes, J. V. A. D. Santos, and A. Katunin. Identification of material properties of a laminated plate from measurements of natural frequencies and modal rotations. *Procedia Structural Integrity*, 17:971–978, 2019. doi: 10.1016/j.prostr.2019.08.129.

[9] J. S. Arora. *Introduction to Optimum Design*. Elsevier, 4^{th} edition, 2004. ISBN: 978-0-12-800806-5.

[10] M. Wahde. *Biologically Inspired Optimization Methods*. WIT, 2008. ISBN: 1845641485.

[11] J. H. Holland. *Adaptation in Natural and Artificial Systems: An Introductory Analysis with Applications to Biology, Control and Artificial Intelligence*. 1975. ISBN: 0-262-58111-6.

[12] X.-S. Yang. *Nature-Inspired Metaheuristic Algorithms Second Edition*. Number May. 2010. doi: 10.1016/j.chemosphere.2009.08.026.

[13] R. Eberhart and J. Kennedy. A New Optimizer Using Particle Swarm Theory. pages 39–43, 1995.

[14] S. Mirjalili, S. M. Mirjalili, and A. Lewis. Grey wolf optimizer. *Advances in Engineering Software*, 69:46 – 61, 2014. doi: 10.1016/j.advengsoft.2013.12.007.

[15] X.-S. Yang. Firefly algorithms for multimodal optimization. In *Proceedings of the 5th International Conference on Stochastic Algorithms: Foundations and Applications*, SAGA'09, page 169–178, Berlin, Heidelberg, 2009. Springer-Verlag.

[16] X.-S. Yang and S. Deb. Cuckoo search via levey flights. pages 210 – 214, 01 2010. doi: 10.1109/NABIC.2009.5393690.

[17] D. Larsson. Using modal analysis for estimation of anisotropic material constants background of proposed modal test method. *Journal of Engineering Mechanics*, 123(9–10):222–229, 1997. report.

[18] F. Igea and A. Cicirello. Part-to-part variability assessment of material properties for flat thin orthotropic rectangular panels using Chladni patterns. *Mechanical Systems and Signal Processing*, 139, 2020. doi: 10.1016/j.ymssp.2019.106559.

[19] ANSYS® mechanical apdl 2020 r1 - theory reference. ansyshelp.ansys.com/, 2020.

[20] K. Hussain, M. N. M. Salleh, S. Cheng, and Y. Shi. Metaheuristic research: a comprehensive survey. *Artificial Intelligence Review*, 52, 2019. doi: 10.1007/s10462-017-9605-z.

[21] J. H. Tam. Identification of elastic properties utilizing non-destructive vibrational evaluation methods with emphasis on definition of objective functions: a review. *Structural and Multidisciplinary Optimization*, 2020. doi: 10.1007/s00158-019-02433-1.

[22] P. Frederiksen. Identification of material parameters in anisotropic plates-a combined numerical/experimental method. *DCAMM Report S*, 60, 1992.